

---

Proceedings of the 37th Polish Seminar on Positron Annihilation, Łądek-Zdrój 2007

# Influence of Ceramic Nanoparticles on Thermal Stability of Ultra Fine Grained Copper

J. ČÍŽEK<sup>a</sup>, I. PROCHÁZKA<sup>a</sup>, M. CIESLAR<sup>a</sup>, R.K. ISLAMGALIEV<sup>b</sup>  
AND O. KULYASOVA<sup>b</sup>

<sup>a</sup>Charles University in Prague, Faculty of Mathematics and Physics  
V Holesovickach 2, CZ-180 00 Praha 8, Czech Republic

<sup>b</sup>Institute of Physics of Advanced Materials

Ufa State Aviation Technical University Ufa 450 000, Russia

A detailed study of the bulk ultra fine grained pure copper and copper with Al<sub>2</sub>O<sub>3</sub> particles was carried out in the present work. The specimens were prepared by the high-pressure torsion and their microstructure was investigated by positron lifetime spectroscopy combined with transmission electron microscopy and microhardness tests. Defects in the as-deformed materials were characterized and the thermal stability of the ultra fine grained microstructure was subsequently examined in annealing experiments. An addition of Al<sub>2</sub>O<sub>3</sub> nanoparticles was found to improve significantly the thermal stability of the ultra fine grained structure, the optimum content of Al<sub>2</sub>O<sub>3</sub> being  $\approx 0.5$  wt.%.

PACS numbers: 78.70.Bj, 79.60.Jv

## 1. Introduction

Ultra fine grained (UFG) metals are distinguished by a mean grain size of the order of several hundreds of nanometers. Many mechanical, thermal, electrical, and other properties of the ordinary polycrystalline metals can be significantly improved by grain refinement down to the UFG region. Hence the structure and properties of the UFG metals are frequently being addressed in the materials studies over the last two decades in order to enhance industrial applications of these materials.

Among the techniques of production of UFG metals, the severe plastic deformation (SPD) seems to be most promising, since it is capable of fabricating bulk amounts of UFG materials of no porosity [1, 2]. High-pressure torsion (HPT) is an SPD technique capable of producing the disk-shaped specimens of a fairly homogeneous UFG structure with a relatively small mean grain size of  $\approx 100$  nm

and a weak texture only [2]. A large amount of defects (dislocations, vacancies, and vacancy clusters) is introduced by SPD. These defects together with grain boundaries (GB's) which become to occupy a significant volume fraction in the UFG materials obviously wield a key influence on formation of the UFG structures and many properties of the SPD-made materials. The SPD process results in a highly non-equilibrium structure. Consequently, the thermal stability of the SPD-created UFG structure becomes a major task of research on these materials.

It is thus obvious that detailed studies of defects and GB's in the SPD-made UFG structures are highly desirable. Positron annihilation spectroscopy (PAS) represents a very useful tool for these investigations [3] since SPD created effects may trap positrons. Moreover, the mean grain size becomes comparable to the positron diffusion length in these systems, so that a large portion of positrons thermalized in the grain interiors may reach GB's by diffusion motion, probing thus the GB's and defects associated with them, too. In many senses, the UFG copper may be regarded as a suitable model system for structure investigations. The temperature development of the microstructure of the *pure* UFG Cu, prepared by HPT, was studied in detail, e.g. [4, 5], and a rather low thermal stability of the UFG microstructure was observed. The grain size resulting from HPT-treated pure Cu was moreover found to vary with the pressure applied in the deformation [5]. However, a reduction in grain size, achieved in this way, leads to a shift of recrystallization onset even to a lower temperature [5].

A relatively low thermal stability of the UFG microstructure, observed for the pure copper, introduces a serious limitation of its use in industrial practice. An addition of ceramic particles seems to be a promising way how to improve thermal stability of the UFG Cu: (i) Ceramic particles are stable up to very high temperatures. (ii) Finely dispersed ceramic particles provide effective obstacles for the movement of dislocations and GB's, hindering thus the grain growth. The effect of addition was demonstrated by us in [6] for the HPT-deformed copper with 0.5 wt.% alumina ( $\text{Al}_2\text{O}_3$ ) nanoparticles.

In the present work, our earlier studies [4–6] of the UFG Cu prepared by HPT will be reviewed and the new investigations on the HPT-deformed Cu with a varying content of alumina nanoparticles will be reported. The main aim of these latest investigations was to find an optimum amount of the alumina additive, which leads to an improvement of thermal stability of the UFG structure in the Cu+ $\text{Al}_2\text{O}_3$  system. The positron lifetime (PL) technique was used as the principal experimental tool in the present work. In addition, direct observations of the microstructure were performed by the transmission electron microscopy (TEM) and the changes of mechanical properties were examined by means of the microhardness measurements.

## 2. Experiment

*Specimens.* The UFG copper specimens were fabricated by HPT deformation of pure Cu (99.99%) and Cu with  $\text{Al}_2\text{O}_3$  nanoparticles (GlidCop). The specimens

were deformed under the pressure of 6 GPa at room temperature up to a true logarithmic strain  $\varepsilon = 7$ . The samples were disk-shaped ( $\approx 10$  mm diameter and  $\approx 0.3$  mm thickness). The three contents of  $\text{Al}_2\text{O}_3$  in Cu were examined: 0.3, 0.5, and 1.1 wt.%. The as-deformed samples were microstructure characterized first. Then they were subjected to a step-by-step isochronal annealing (an effective heating rate of  $1^\circ\text{C}/\text{min}$ ). Each annealing step was finished by a rapid quenching in the water of room temperature and the microstructure characterizations were performed at room temperature.

*Measurements.* The PL measurements were carried out by means of the fast-fast configuration of a  $\text{BaF}_2$  spectrometer [7]. A  $\approx 1.3$  MBq of  $^{22}\text{Na}_2\text{CO}_3$  (iThemba Labs) deposited between two mylar C foils (Dupont) of  $\approx 2.5$   $\mu\text{m}$  thickness was used as a positron source. The diameter of the positron source spot was  $\approx 4$  mm. Using this source, the spectrometer gave a time resolution of 160 ps for  $^{22}\text{Na}$  (FWHM) at a count rate of  $120\text{ s}^{-1}$  for the 1274–511 keV coincidences. At least  $10^7$  counts were accumulated in each measured PL spectrum. The spectra were decomposed into up to the four exponential components using a maximum-likelihood based procedure [7].

The TEM observations were carried out using a JEOL 2000 FX electron microscope operating at 200 kV. The Vicker microhardness (HV) measurements were performed using a LECO M-400-A hardness tester with a load of 100 g applied for 10 s.

### 3. Results and discussion

*As deformed structure.* The TEM results of the present work are illustrated in Fig. 1. The as-deformed UFG Cu+ $\text{Al}_2\text{O}_3$  specimens exhibited virtually the same microstructure as the UFG pure Cu HPT-deformed under 6 GPa which has been studied in detail in [4, 5]. It is highly fragmented, characterized by a mean grain size of  $\approx 150$  nm, and contains mostly high-angle type GB's and a high density of dislocations. The spatial distribution of dislocations is moreover strongly non-uniform. Dislocations are concentrated mainly in the distorted layers along the GB's, while the grain interiors remain almost free of dislocations. The TEM observations of alumina particles revealed the two kinds of  $\text{Al}_2\text{O}_3$  particles: (i) the isolated "coarse" particles with a size of  $\approx 100$  nm and (ii) the clumps of very fine nanoparticles with a diameter of  $\leq 10$  nm.

The torsion deformation-induced strains increase from the center of the sample to its edge. Therefore, the defect density may be expected to depend on radial distance  $r$  from the sample center. This supposition was examined using the microhardness measurements on the pure UFG Cu and UFG Cu+0.5 wt.%  $\text{Al}_2\text{O}_3$ . The results of these measurements are presented in Fig. 2a. Significantly higher values of microhardness, HV, are observed for the specimen with alumina particles than that for the pure Cu. Thus, as expected, alumina particles cause a significant hardening in addition to that caused by grain refinement and a high dislocation

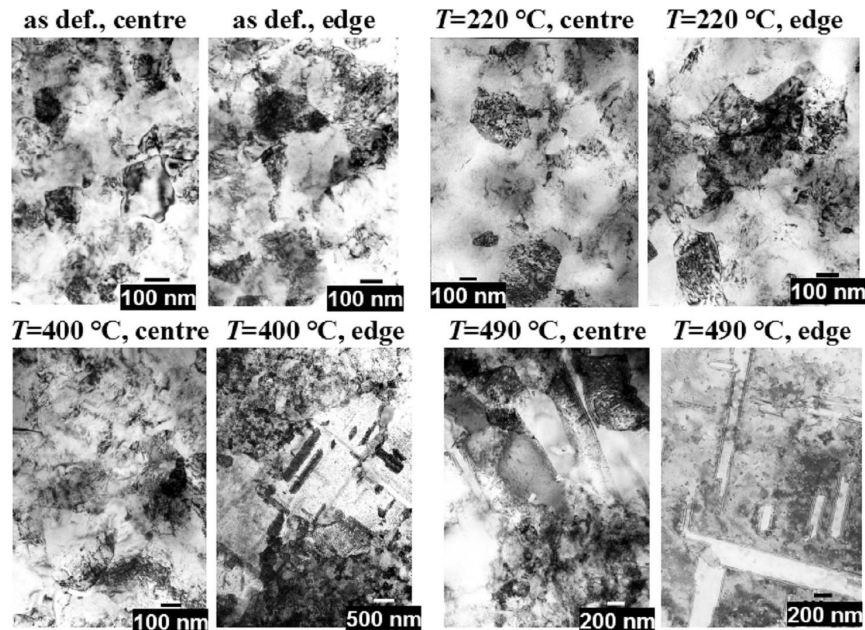


Fig. 1. The bright field TEM images for the UFG Cu+0.5 wt.% Al<sub>2</sub>O<sub>3</sub> at the central part and the edge of the specimen ( $r = 4$  mm radial distance). Annealing temperatures are shown in the figure.

density. Moreover, an increase in HV with radius  $r$  was observed for both the samples, see Fig. 2a. It indicates an increase in the average dislocation density from the center of the sample towards its edge. Hence, the center of the sample exhibits the lowest dislocation density, while the highest number of dislocations can be found at the sample edge. Such a lateral distribution of dislocations seems to be typical of HPT-deformed UFG metals.

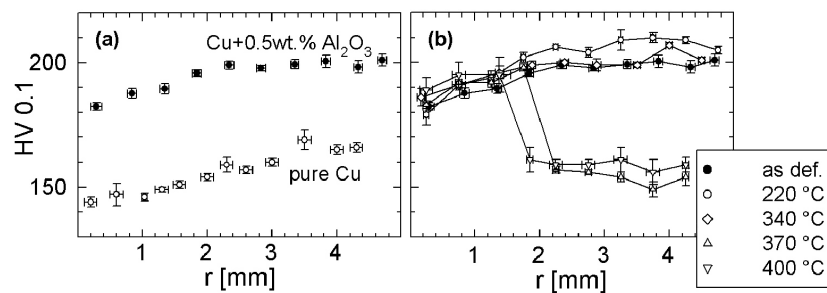


Fig. 2. The dependence of microhardness, HV, on radial distance,  $r$ , from the sample center: (a) the comparison of the as-deformed UFG pure Cu and Cu+0.5 wt.% Al<sub>2</sub>O<sub>3</sub>, (b) the evolution of microhardness during annealing for the UFG Cu+0.5 wt.% Al<sub>2</sub>O<sub>3</sub>.

The two components could be resolved in measured PL spectra of the as-deformed specimens (beside the components arising from the contribution of positrons annihilating in the source salt and the covering foils). The measured values of lifetimes,  $\tau_i$ , and relative intensities,  $I_i$ ,  $i = 2, 3$ , are listed in Table. Both these lifetimes lie significantly above the known bulk lifetime for a well-annealed pure copper,  $\tau_b = 114.8$  ps [8]. It indicates a saturated trapping of positrons in defects in the as-deformed UFG specimens. A majority of positrons are trapped at dislocations in the distorted regions along the GB's (lifetime  $\tau_2 \approx 164$  ps). The longer components with lifetimes  $\tau_3 \approx 250$  ps come from positrons trapped in small vacancy clusters (microvoids) situated inside grains. The size of the microvoids was deduced from the observed  $\tau_3$  values. It is equivalent to  $4 \div 5$  vacancies in the UFG pure Cu. Let us note that  $\tau_3$  values for Cu+Al<sub>2</sub>O<sub>3</sub> samples in Table are slightly higher than  $\tau_3$  for the UFG pure Cu indicating thus slightly larger microvoids,  $6 \div 7$  vacancies. Arguments supporting the interpretation of the  $\tau_2$  and  $\tau_3$  components were discussed in detail in our earlier works on the pure UFG Cu [4, 5]. *Thermal stability of UFG structure.* In Refs. [4, 5] we have performed

TABLE

Positron lifetimes  $\tau_i$  and relative intensities  $I_i$  ( $i = 2, 3$ ) observed in as-deformed samples. The one standard deviations are given in parentheses in the units of the last significant digits.

Sample	$\tau_2$ [ns]	$I_2$ [%]	$\tau_3$ [ns]	$I_3$ [%]
pure Cu	0.164(1)	83(5)	0.255(4)	17(3)
Cu+0.3wt.%Al <sub>2</sub> O <sub>3</sub>	0.166(1)	80(1)	0.295(5)	20(1)
Cu+0.5wt.%Al <sub>2</sub> O <sub>3</sub>	0.165(2)	71(1)	0.301(4)	29(1)
Cu+1.1wt.%Al <sub>2</sub> O <sub>3</sub>	0.166(1)	70(1)	0.297(3)	30(1)

detailed PAS and TEM investigations of the thermal stability of UFG structure in the HPT-deformed pure Cu. The results of may be summarized on the following lines: (i) The recovery of the UFG structure starts from the abnormal grain growth when isolated recrystallized grains appear in virtually unchanged matrix. (ii) At higher temperatures, the abnormal grain growth stage passes to the recrystallization, in which grain growth occurs in the whole volume of the material. Recrystallization onsets at  $\approx 190^\circ\text{C}$  [5].

The PL parameters were measured as functions of the annealing temperature for all the three UFG Cu+Al<sub>2</sub>O<sub>3</sub> systems studied in the present work and the results obtained are shown in Fig. 3. A comparison with the pure UFG Cu is given for relative intensities in Fig. 3b, too. One can see from Fig. 3a that the two lifetimes of  $\tau_2 \approx 164$  ps and  $\tau_3 \approx 290$  ps, are found also in all the three Cu+Al<sub>2</sub>O<sub>3</sub> systems and remain almost unchanged throughout the whole region of annealing temperatures. Obviously, these two components arise from positrons

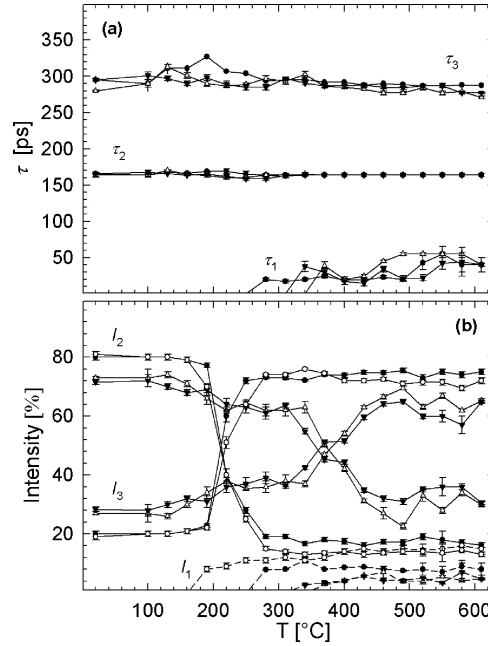


Fig. 3. The variations of positron lifetimes  $\tau_i$  (a) and intensities  $I_i$  (b),  $i = 1, 2, 3$ , during isochronal annealing:  $\bullet$  — 0.3 wt.% Al<sub>2</sub>O<sub>3</sub>,  $\triangle$  — 0.5 wt.% Al<sub>2</sub>O<sub>3</sub>,  $\blacktriangledown$  — 1.1 wt.% Al<sub>2</sub>O<sub>3</sub>,  $\circ$  — pure Cu.

trapped at dislocations in distorted regions close to the GB's and in the microvoids, respectively. An additional component appears at higher annealing temperatures. Its lifetime  $\tau_1 < \tau_b$  clearly show this component to be attributed to annihilations of free positrons. A strong decrease in intensity  $I_2$  belonging to positrons trapped at dislocations is apparent in Fig. 3b for both the pure UFG Cu and Cu+Al<sub>2</sub>O<sub>3</sub>. Such a decrease is a distinct indication of recrystallization, because the distorted regions with a high dislocation density along GB's are replaced by recrystallized grains, which are almost free of dislocations. The increase in intensity  $I_3$  seen from Fig. 3b is then understood as a consequence of intensity normalization rather than a real increase in the concentration of microvoids. The pure UFG Cu exhibits a drastic decrease in  $I_2$ , i.e. the recrystallization onset, starting at 190°C. On the other hand, the UFG Cu with 0.5 wt.% of Al<sub>2</sub>O<sub>3</sub> exhibits only a slight drop of  $I_2$  around 200°C, which is likely due to some rearrangement and/or a partial annihilation of dislocations and a sharpening of the distorted regions. The microstructure of this sample remains essentially unchanged up to 340°C, as demonstrated by the behavior of  $I_2$  in Fig. 3b. Again, a strong decrease in  $I_2$  above 340°C indicates the onset of recrystallization in the UFG Cu+0.5 wt.% Al<sub>2</sub>O<sub>3</sub>, which is by 150°C higher than in the pure UFG Cu.

An above information gained from the PL measurements of annealing curves was supplemented by TEM observations on the UFG Cu with 0.5 wt.% of  $\text{Al}_2\text{O}_3$  at 220, 400, and 490°C. The corresponding TEM images are included in Fig. 1. An intensive grain growth was observed by TEM in the pure UFG Cu annealed up to 220°C, see Ref. [4]. On the other hand, no grain growth was observed by TEM on the UFG Cu+0.5 wt.%  $\text{Al}_2\text{O}_3$  at this temperature, see Fig. 1. TEM images, taken from the centre and the edge of the UFG Cu with 0.5 wt.%  $\text{Al}_2\text{O}_3$  annealed up to 400°C (Fig. 1) clearly demonstrate that recrystallization takes place at the edge, while a basically unchanged structure was observed in the center. It gives an obvious evidence that recrystallization begins at the edge of the sample. Such a phenomenon can be understood taking into account that the HPT deformation-induced strain increases from the center towards the edge of the sample. Hence, there is more deformation energy stored at the margin than at the center of the sample. The driving force for the recovery of the UFG structure is then higher at the margins and recrystallization starts from the edge of the sample. At higher annealing temperatures, the recrystallized region penetrates towards the central part of the sample. This is demonstrated by the corresponding TEM images in Fig. 1, in which the microstructure of the central and edge regions for the UFG Cu with 0.5 wt.%  $\text{Al}_2\text{O}_3$  annealed up to 490°C is shown. Grain growth is now apparent also in the sample center, although it yet exhibits only a partially recovered structure with recrystallization being still in progress. On the other hand, a completely recrystallized structure is seen at the sample edge at 490°C annealing temperature.

A further evidence of a centripetal recrystallization is provided by microhardness measurements as functions of the radial distance  $r$  and the annealing temperature. These are plotted in Fig. 3b for temperatures of 220, 340, 370, and 400°C. A drop in HV from values characteristic of a well developed UFG structure (up to 340 °C) to the recrystallized one is seen at 370 and 400°C, whereas the drop is shifted towards the center for the higher temperature.

*Optimization of  $\text{Al}_2\text{O}_3$  content.* The dependences of the PL parameters on annealing temperature were measured for the other two UFG Cu+ $\text{Al}_2\text{O}_3$  specimens studied in the present work, too, see Fig. 3. On the basis of the data on  $I_2$  given in Fig. 3b, we utilize the decrease in  $I_2$  as an indication of the recrystallization onset. It can be seen from the figure that only a minor improvement of the recrystallization onset temperature, compared to the pure UFG Cu case, is achieved for the UFG Cu+0.3 wt.%  $\text{Al}_2\text{O}_3$ , whereas substantially higher onset temperatures are found for the other two  $\text{Al}_2\text{O}_3$  contents, the  $I_2$ -curves being practically identical for the two systems. One can conclude from this fact that an optimum amount of  $\text{Al}_2\text{O}_3$  particles added to Cu in order to reach a maximum improvement of the thermal stability of the Cu+ $\text{Al}_2\text{O}_3$  UFG structure lies around 0.5 wt.%.

#### 4. Conclusions

The bulk UFG pure copper and copper with Al<sub>2</sub>O<sub>3</sub> particles were prepared by the high-pressure torsion and their microstructure was investigated by PL spectroscopy combined with transmission electron microscopy and microhardness tests. The as-deformed specimens exhibited a highly fragmented structure with mainly high-angle type GB's, a mean grain size of  $\approx 150$  nm and a high average dislocation density. The average dislocation density was found to increase with radial distance from the sample center. A strongly non-homogeneous spatial distribution of dislocations was observed. Dislocations are concentrated in the distorted regions along GB's, while grain interiors are almost free of dislocations. Microvoids equivalent in size to 6 ÷ 7 vacancies in UFG Cu with Al<sub>2</sub>O<sub>3</sub> nanoparticles and 4 ÷ 5 vacancies in pure UFG Cu were also identified.

The thermal stability of the UFG Cu and Cu+Al<sub>2</sub>O<sub>3</sub> structures with the mean grain size of  $\approx 150$  nm was examined in isochronal annealing experiments. It was found that an addition of Al<sub>2</sub>O<sub>3</sub> nanoparticles improves significantly the thermal stability of the UFG structure, the optimum content of Al<sub>2</sub>O<sub>3</sub> being  $\approx 0.5$  wt.%.

#### Acknowledgments

This work was financially supported from the Czech Science Foundation under contract No. GA 106/05/0073 and from the Ministry of Education, Youth and Sports of the Czech Republic (scientific plan MS 0021620834).

#### References

- [1] *Nanomaterials by Severe Plastic Deformation, Proc. Int. Conf. "Nanomaterials by Severe Plastic Deformation — NANOSPD2", Vienna 2002*, Eds. M. Zehetbauer, R.Z. Valiev, Wiley-VCH Verlag GmbH&Co. KGaA, Weinheim 2004.
- [2] R.Z. Valiev, R.K. Islamgaliev, V.S. Aleksandrov, *Prog. Mater. Sci.* **45**, 103 (2000).
- [3] P. Hautojrvi, C. Corbel, in: *Positron Spectroscopy of Solids, Proc. Int. School of Physics .Enrico Fermi/, Course CXXV, Varenna (Italy) 1993*, Eds. A. Dupasquier, A.P. Mills, Jr., IOS Press, Amsterdam 1995, p. 491.
- [4] J. Cizek, I. Prochazka, M. Cieslar, R. Kuzel, J. Kuriplach, F. Chmelik, I. Stulikova, F. Becvar, O. Melikhova, R.K. Islamgaliev, *Phys. Rev. B* **65**, 094106 (2002).
- [5] J. Cizek, I. Prochazka, R. Kuzel, M. Cieslar, R.K. Islamgaliev, *J. Metastable Nanocryst. Mater.* **17**, 37 (2003).
- [6] J. Cizek, I. Prochazka, R. Kuzel, R.K. Islamgaliev, *Chemical Monthly* **133**, 873 (2002).
- [7] F. Becvar, J. Cizek, L. Lestak, I. Novotny, I. Prochazka, F. Sebesta, *Nucl. Instrum. Methods Phys. Res. A* **443**, 557 (2000).
- [8] J. Cizek, I. Prochazka, P. Vostry, F. Chmelik, R.K. Islamgaliev, *Acta Phys. Pol. A* **95**, 487 (1999).